Major Groove Interactions of Vaccinia Topo I Provide Specificity by Optimally Positioning the Covalent Phosphotyrosine Linkage†

Rajesh Nagarajan and James T. Stivers*

Department of Pharmacology and Molecular Sciences, The Johns Hopkins University School of Medicine, 725 North Wolfe Street, Baltimore, Maryland 21205-2185

Received January 20, 2006; Revised Manuscript Received March 7, 2006

ABSTRACT: Vaccinia DNA topoisomerase (vTopo) is a prototypic eukaryotic type I topoisomerase that shows high specificity for nucleophilic substitution at a single phosphodiester linkage in the pentapyrimidine recognition sequence 5′-(C/T)$^{+5}$C^{+4}C^{+3}T^{+2}T^{+1}p↓N^{-1}. This reaction involves reversible transesterification where the active site tyrosine of the enzyme and a 5′-hydroxyl nucleophile of DNA compete for attack at the phosphoryl group. The finite lifetime of the covalent phosphotyrosine adduct allows the enzyme to relax multiple supercoils by rotation of the 5′-OH strand before the DNA backbone is religated. To dissect the nature of the unique sequence specificity, subtle modifications to the major groove of the GGGAA 5′-sequence of the nonscissile strand were introduced and their effects on each step of the catalytic cycle were measured. Although these modifications had no effect on noncovalent DNA binding (K_D) or the rate of reversible DNA cleavage (k_{cl}), significant decreases in the cleavage equilibrium ($K_{cl} = k_{cl}/k_r$) arising from increased rates of 5′-hydroxyl attack (k_r) at the phosphotyrosine linkage were observed. These data and other findings support a model in which major groove interactions are used to position the phosphotyrosine linkage relative to the mobile 5′-hydroxyl nucleophile. In the absence of native sequence interactions, the phosphotyrosine has a higher probability of encountering the 5′-hydroxyl nucleophile, leading to an enhanced rate of ligation and a diminished equilibrium constant for cleavage. By this unusual specificity mechanism, the enzyme prevents formation of stable covalent adducts at nonconsensus sites in genomic DNA.

Vaccinia virus topoisomerase I (vTopo)[1] and other eukaryotic type IB enzymes maintain DNA topology by relaxing superhelical tension in DNA. The Topo reaction is comprised of multiple steps as shown in Figure 1: (i) noncovalent binding of the enzyme to duplex DNA with a dissociation constant K_D, (ii) cleavage of a single DNA strand by an active site tyrosine nucleophile leading to formation of a covalent 3′-phosphotyrosyl linkage and a free 5′-hydroxyl (k_{cl}), (iii) release of superhelical tension by a strand rotation mechanism (k_{sup}), and (iv) religation of the DNA break by attack of the 5′-hydroxyl nucleophile (k_r). Vaccinia topoisomerase is unique among these enzymes in that it exhibits high specificity for cleavage at the consensus pentapyrimidine sequence 5′-(C/T)CCTT↓ (*1*−*8*). However, the remarkable site specificity of vTopo is not understood at the molecular level because the holoenzyme has proven to be refractory to crystallization, necessitating the application of other approaches for elucidation of this question.

One way to define specificity for vTopo is to compare the efficiency of forming the covalent adduct at the consensus site to that at another site that differs from the consensus sequence. Sequence-specific interactions within the consen-

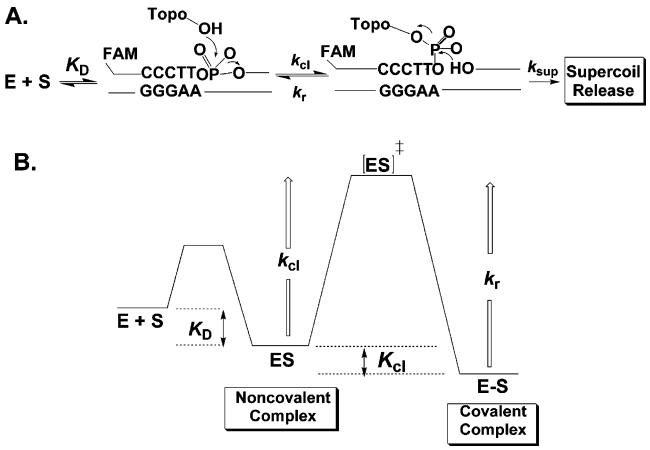

FIGURE 1: Topoisomerase reaction cycle. (A) The three steps in the vTopo reaction are DNA binding, reversible DNA backbone cleavage described by the rate constants k_{cl} and k_r, and, for supercoiled DNA substrates, supercoil relaxation while the enzyme is covalently attached to the phosphodiester backbone (k_{sup}). Relaxation occurs by a "free rotation" mechanism in which the noncovalently bound end swivels around the helix axis. The number of supercoils that are removed after a single cleavage event is dependent on the k_{sup}/k_r ratio: if k_r is rapid, there is no opportunity for DNA rotation before the strand is resealed. (B) Free energy reaction coordinate profile depicting the thermodynamic and kinetic barriers of the reaction. The rate constants and equilibrium constants refer to the free energy barriers defined by the relations $K = \exp(-\Delta G/RT)$ and $k = (k_B T/h)\exp(-\Delta G^{\ddagger}/RT)$.

† This work was supported by National Institutes of Health Research Grant GM 68626 (J.T.S.).

* To whom correspondence should be addressed: Department of Pharmacology and Molecular Sciences, The Johns Hopkins University School of Medicine, 725 N. Wolfe St., Baltimore, MD 21205-2185. Telephone: (410) 502-2758. Fax: (410) 955-3023. E-mail: jstivers@jhmi.edu.

[1] Abbreviations: vTopo, vaccinia DNA topoisomerase IB; FAM, 6-carboxyfluorescein; N, 2-aminopurine; P, purine; B, deazaadenine; H, deazaguanine; buffer A, 20 mM Tris-HCl, 200 mM NaCl, and 1 mM DTT (pH 8.0).

10.1021/bi060133i CCC: $33.50
Published on Web 04/11/2006

sus sequence are used to kinetically or thermodynamically facilitate the formation of the enzyme−DNA covalent adduct, whereas alternative sequences cannot realize the same benefit, resulting in specificity. This is a useful definition because the lifetime (or concentration) of the covalent phosphotyrosine adduct largely determines how efficiently the enzyme removes supercoils from DNA using a strand rotation mechanism as defined in the legend of Figure 1A (*9*, *10*).

Using this definition, specificity can be achieved at one of three stages of the reaction (Figure 1B). If strong sequence-specific enzyme−DNA interactions are used only to discriminate at the noncovalent binding step (ES, Figure 1B), then the relative amount of covalent adduct at the specific sequence would be increased relative to the that at the nonspecific sequence because the specific site has a higher occupancy. This follows because the relative amount of covalent adduct is determined by the K_{cl}/K_D ratio. (This analysis makes the limiting assumption that K_{cl} is the same for the specific and nonspecific substrates.) Alternatively, interactions of the enzyme with the consensus site could be weak in the noncovalent complex and then become strong at the transition state for cleavage ($ES^{‡}$, Figure 1B). In this case, the activation barrier for cleavage is lowered in the presence of the consensus interactions, thereby increasing the rate of formation of the covalent adduct (E−S, Figure 1). In this regard, many of the direct enzyme catalytic interactions with the phosphoryl group have been found to act solely by transition state stabilization (*11*). However, transition state stabilization by itself is unsatisfactory for specificity because it would also give rise to a decrease in the lifetime of the covalent intermediate at the specific site. This follows because stabilization of $ES^{‡}$ has an equal effect on enhancing the rates of both cleavage and ligation: as the religation rate increases, fewer supercoils are removed each time the covalent complex is formed, resulting in decreased specificity by our definition. Finally, if sequence-specific interactions are used to stabilize the covalent complex (E−S, Figure 1), then its relative concentration would be greater at consensus sites, generating specificity (Figure 1B). It is clear from this analysis that an understanding of specificity requires measurements of the relative strength of interactions in the ES, $ES^{‡}$, and E−S complexes as a function of discrete changes in the consensus DNA sequence.

Previous footprinting, chemical protection/interference, and UV cross-linking studies have indicated that vTopo makes contacts within the major groove of the GGGAA sequence of the nonscissile strand (*4*, *7*, *12*−*14*). For instance, site-specific modification with benzo[*c*]phenanthrene at N2 and N6 of G can reduce the cleavage rate by a factor of 1000 (*6*), and site-specific modification of the exocylic amino groups of the adenines at positions 1 and 2 with benzo[*a*]-pyrene decreased the rate of cleavage by approximately 10^3-fold (*15*). The rate effects on strand cleavage arising from the more subtle major groove modifications of 8-oxoguanine, 8-oxoadenine, and 2-aminopurine have also been explored, where deleterious effects as large as 35-fold at G^{+3} were observed (*15*). In addition, stereospecific methylphosphonate substitutions of the nonbridging phosphate oxygens in the DNA backbone of this sequence have highlighted the significance of major and minor groove electrostatic interactions toward sequence-specific recognition (*8*). Although these previous findings highlight the significance of major groove interactions, the discrete energetic role of the hydrogen bonding groups that are presented within the major groove of the GGGAA sequence has never been evaluated at each step along the reaction coordinate.

In this paper, we describe a study in which the N7 hydrogen bond acceptor groups of each guanine and adenine within the consensus sequence are replaced with unnatural 7-deaza bases. In separate experiments, the individual guanine O6 and adenine N6 groups are removed for investigation of hydrogen bonding at these major groove positions (Figure 2). Systematic dissection of the energetics of these changes at each step along the reaction pathway shows that major groove hydrogen bonds are in general used to increase the stability of the covalent E−S complex, without having any energetic effect on the noncovalent or transition state complexes (Figure 1B). A reasonable physical interpretation is that these interactions are used to optimally position the covalent phosphotyrosine linkage relative to the attacking 5′-hydroxyl nucleophile.

MATERIALS AND METHODS

Enzymes. The cloning and purification of wild-type vaccinia topoisomerase have been previously described (*16*). The enzyme concentration was determined by UV absorption using an extinction coefficient of 41 797 M^{-1} cm^{-1} in a buffer containing 20 mM sodium phosphate at pH 6.0.

DNA Substrates with Fluorescent Tags. The sequence of the 32-mer DNA substrate containing the consensus cleavage sequence is shown in Figure 2, where FAM is 6-carboxy-fluorescein. The synthesis of the nonscissile strand with modified bases incorporated at various sites was accomplished by substituting the modified base during DNA synthesis at these positions. All oligonucleotides were synthesized using an ABI 394 synthesizer using nucleoside phosphoramidites obtained from Glen Research. The oligonucleotides were purified using anion exchange HPLC and then desalted using C-18 reverse phase chromatography. The purity of oligonucleotides was confirmed using electrophoresis through a 20% polyacrylamide gel containing 7 M urea and MALDI-TOF analysis. The DNA duplexes were prepared in buffer A [20 mM Tris-HCl, 200 mM NaCl, and 1 mM DTT (pH 8.0)] by mixing the two strands in a molar ratio of 1:2 (nonscissile strand in excess).

Equilibrium Cleavage Measurements. The equilibrium cleavage measurements were performed using buffer A by titrating FAM32AP/32-mer (60 nM) with increasing concentrations of Topo (40−600 nM). The covalent complex was trapped by the addition of 1 volume of 10% SDS after 1 h. The fraction covalent complex at each enzyme concentration [counts in covalent complex/(counts in covalent complex + counts in free DNA)] was quantified using ImageQuant. The fraction covalent complex was plotted against enzyme concentration to obtain the values of the binding constant (K_D) and cleavage−religation equilibrium constant (K_{cl}) using the following equation (eq 1) (*16*).

$$\text{fraction of complex} = \frac{b - \sqrt{b^2 - 4a^2[\text{E}][\text{S}]}}{2a^2[\text{S}]} \quad (1)$$

where $a = 1 + 1/K_{cl}$, $b = a[\text{E}] + a[\text{S}] + K_D/K_{cl}$, $K_{cl} =$

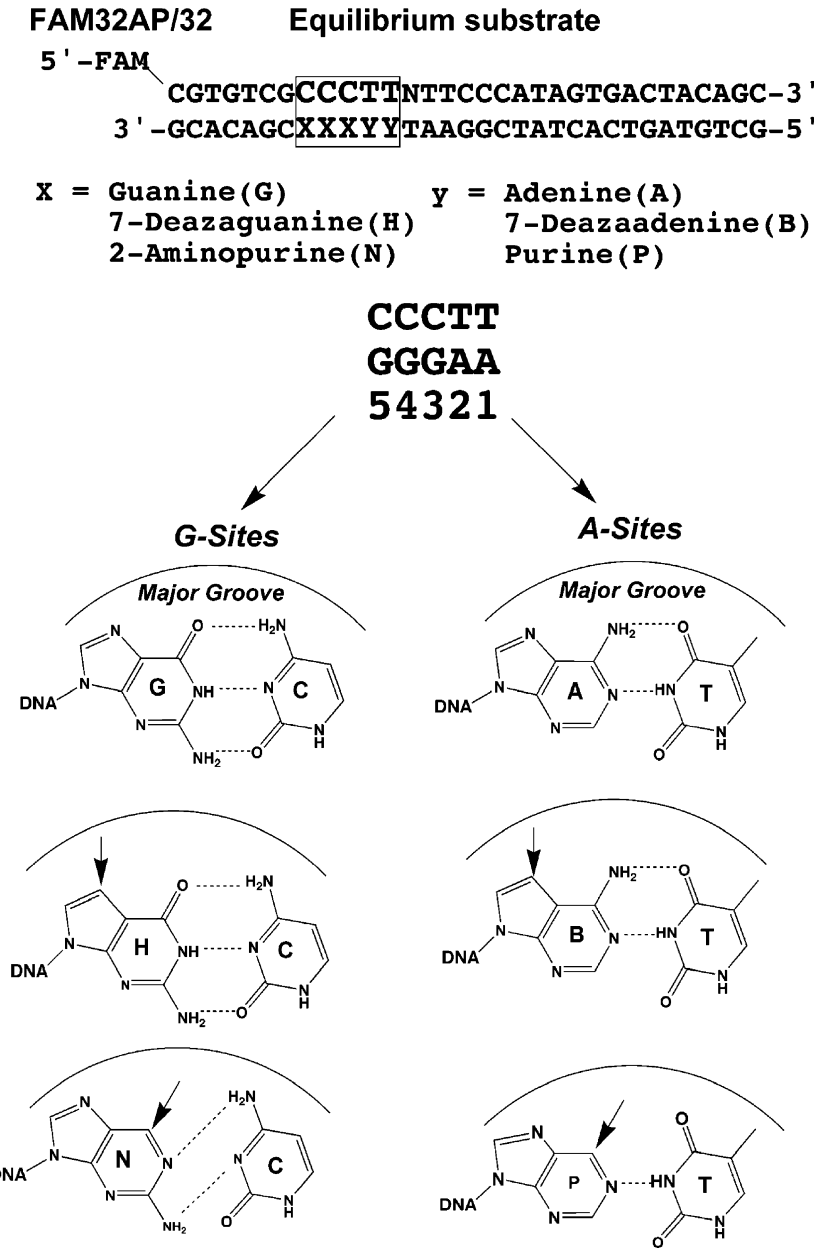

FIGURE 2: DNA substrate used in this study. The normal G·C and A·T base pairs of the consensus sequence were replaced with unnatural bases in the GGGAA sequence of the consensus site. The arrows indicate potential contact points that are absent with the modified bases. The 7-deaza modification does not affect base pairing, whereas N and P disrupt the hydrogen bonding of the base pair.

k_{cl}/k_r, and [E] and [S] are the total enzyme and substrate concentrations, respectively. In this analysis, the counts that migrate as free DNA represent the sum of the counts that were bound noncovalently to the enzyme and those of the unbound DNA. All measurements were repeated two or three times to estimate errors.

Approach to Equilibrium Kinetics. The rate constant for approach to equilibrium in a FAM32AP/32-mer substrate was measured using a KinTek rapid quench instrument. The final enzyme and DNA concentrations were kept at 1 μM and 100 nM, respectively. The enzyme and DNA were mixed, and the reactions were quenched using 10% SDS at time intervals ranging between 2.5 and 750 ms. The samples were subjected to electrophoresis on a 10% SDS−PAGE gel. The 6-FAM fluorophore in the free DNA and enzyme−DNA covalent adduct was quantified using a Typhoon scanner. Since the dye front ran along with the free DNA band, giving rise to inner filter effects, the samples were loaded onto the gel without the dye component. The fraction of covalent complex formed at each time was fitted to a first-order rate equation to obtain k_{obs} which equals the sum of the cleavage and religation rate constants (i.e., $k_{obs} = k_{cl} + k_r$) (*16*). Thus, using the K_{cl} obtained from equilibrium cleavage measurements, the cleavage and religation rate constants (k_r) may be calculated using the equations $k_{cl} = k_{obs}/(1/K_{cl} + 1)$ and $k_r = k_{obs}/(K_{cl} + 1)$. All measurements were repeated two or three times to estimate errors.

RESULTS

Overall Approach. We sought to evaluate the energetic role of interactions of vTopo with the DNA major groove by introducing subtle site-specific modifications within the $G^{+5}G^{+4}G^{+3}A^{+2}A^{+1}$ sequence in the nonscissile strand as shown in Figure 2. In the nomenclature used here, the identity

Table 1: Nomenclature, DNA Sequences, and Kinetic and Thermodynamic Parameters for the Major Groove-Modified DNAs[a]

DNA	sequence	K_D (nM)	K_{cl}	k_{cl} (s^{-1})	k_r (s^{-1})
unmodified	GGGAA	118 ± 25	1.6 ± 0.3	2.2 ± 0.2	1.4 ± 0.2
B1	GGGA**B**	94 ± 46	0.8 ± 0.2	2.8 ± 0.3	3.5 ± 0.3
B2	GGG**B**A	74 ± 22	0.7 ± 0.1	2.2 ± 0.1	3.0 ± 0.2
P1	GGGA**P**	64 ± 21	1.5 ± 0.3	2.5 ± 0.2	1.7 ± 0.2
P2	GGG**P**A	72 ± 15	2.7 ± 0.6	3.1 ± 0.2	1.1 ± 0.2
H3	GG**H**AA	77 ± 26	0.7 ± 0.1	3.2 ± 0.2	4.4 ± 0.2
H4	G**H**GAA	59 ± 14	0.5 ± 0.03	1.6 ± 0.1	3.4 ± 0.1
H5	**H**GGAA	75 ± 16	0.4 ± 0.03	1.5 ± 0.1	4.2 ± 0.1
N3	GG**N**AA	55 ± 21	1.0 ± 0.2	3.2 ± 0.2	3.2 ± 0.2
N4	G**N**GAA	171 ± 21	0.5 ± 0.03	2.4 ± 0.1	5.1 ± 0.1
N5	**N**GGAA	148 ± 32	0.5 ± 0.05	2.3 ± 0.1	4.8 ± 0.1
B2B1	GGG**BB**	80 ± 17	2.1 ± 0.4	4.7 ± 0.2	2.2 ± 0.2
H5H4	**HH**GAA	67 ± 21	0.5 ± 0.06	2.7 ± 0.1	5.8 ± 0.1
H5H3	**H**G**H**AA	110 ± 21	0.3 ± 0.02	0.9 ± 0.1	3.1 ± 0.2
N5N4	**NN**GAA	87 ± 14	0.1 ± 0.005	0.2 ± 0.1	2.5 ± 0.3
N5N3	**N**G**N**AA	48 ± 18	0.2 ± 0.02	1.1 ± 0.2	4.8 ± 0.2
H3B1	GG**H**A**B**	72 ± 21	1.5 ± 0.3	2.2 ± 0.2	1.5 ± 0.2
N4B1	G**N**GA**B**	193 ± 21	0.7 ± 0.05	5.3 ± 0.1	7.7 ± 0.1

[a] See Figure 2 for structures of B, H, P, and N.

and position of the substituted base are given by a letter and number, respectively, where H is 7-deazaguanine, N is 2-aminopurine, B is 7-dezaadenine, and P is purine. Thus, substitution of 7-dezaguanine at position 5 would be represented as N5, and double N substitutions at positions 4 and 5 would be designated N5N4. The 17 single and double DNA substitutions that were synthesized and studied in this work are listed in Table 1. These sequences show H and N substitutions in each of the G positions, B and P substitutions in both of the A sites, and combined H, B and N, B substitutions at both the G and A sites.

Because these modifications result in very subtle changes in structure, we anticipated kinetic and thermodynamic consequences of <10-fold in the various reaction parameters of vTopo. Accordingly, accurate and precise measurements of K_D, K_{cl}, k_{cl}, and k_r were required. A new experimental protocol is used here that meets this requirement. This new method has several advantages over previous approaches, including (i) the use of a nonradioactive 5′-fluorescein probe, (ii) measurement of the noncovalent binding constant (K_D) using the wild-type enzyme instead of the Y274F surrogate that lacks the covalent nucleophile (*16*), and (iii) measurement of K_D, k_{cl}, k_r, and K_{cl} using a single approach-to-equilibrium substrate. This new method requires only two experiments to obtain all of these reaction parameters: an equilibrium measurement of both K_D and K_{cl} and a kinetic measurement of the observed rate constant for the approach to equilibrium ($k_{obs} = k_{cl} + k_r$). Although only two experiments are required, these parameters are robustly determined by these measurements. In the equilibrium measurement of K_D and K_{cl}, the concentration dependence for formation of the covalent complex assesses the preequilibrium formation of the noncovalent complex ($K_D = [E][S]/[ES]$), and the end point provides a direct measurement of the internal equilibrium ($K_{cl} = [E{-}S]/[ES]$). For an approach to equilibrium involving two species (in this case, ES and E−S), only two of the three measurable parameters (k_{cl}, k_r, and K_{cl}) are required for characterization of the system because once two are known, the other may be calculated using the equation $K_{cl} = k_{cl}/k_r$. The validity of the two-state approximation, and confirmation of the agreement between approach-to-equilibrium and irreversible reaction kinetic measurements, have been confirmed in previous studies (*11*, *16*−*18*). We show representative data using this approach in the Results and then interpret the findings in the Discussion on the basis of the full results which are summarized in Table 1.

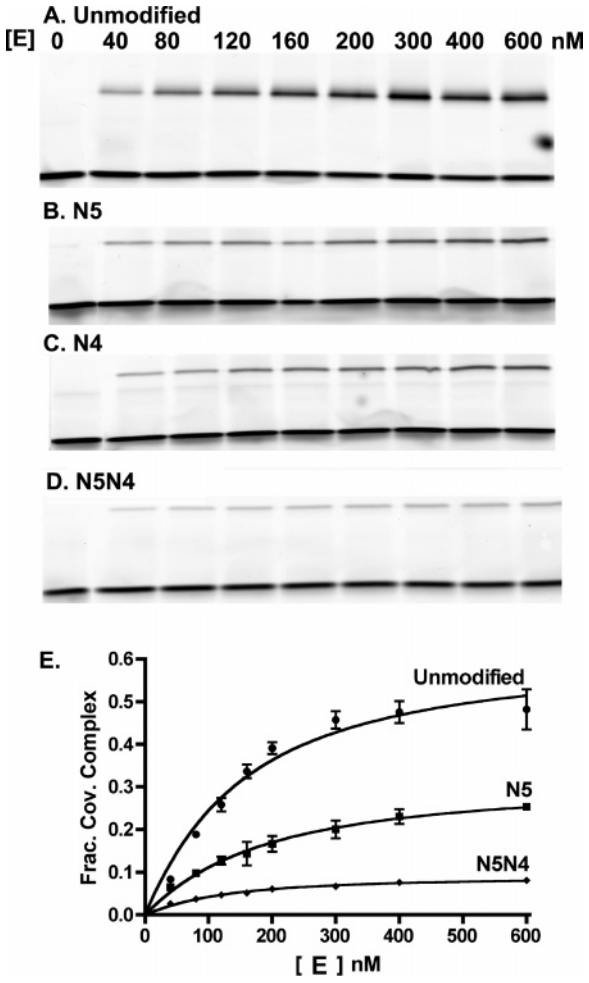

FIGURE 3: Equilibrium cleavage of the FAM32AP/32-mer duplex DNA. (A−D) SDS−PAGE gels showing the equilibrium reactions of vTopo with unmodified, singly modified (N5 and N4), and doubly modified (N5N4) DNA as a function of enzyme concentration. The top band in each panel is the E−S covalent complex, whereas the bottom band is the free DNA. (E) Plotting the fraction of covalent complex vs vTopo concentration and fitting to eq 1 provide the binding constant (K_D) and the cleavage equilibrium constant (K_{cl}) for these DNA substrates.

Binding Constant (K_D) and Cleavage Equilibrium Constant (K_{cl}). Both K_D and K_{cl} were determined from a single experiment by titrating a limiting concentration of DNA with excess Topo. As the enzyme concentration is increased, more of the free DNA is bound noncovalently, and by mass action, more covalent complex is formed as well. Thus, upon adding SDS to trap the equilibrium amount of the covalent complex at each enzyme concentration and resolving the covalent complex from the free DNA by denaturing gel electrophoresis, we extracted the binding and internal cleavage equilibria from the data using eq 1. As shown in Figure 3A−D for the native DNA and for the three modified sequences (N4, N5, and N5N4, respectively), the enzyme−substrate covalent complex (upper band) and the free DNA (lower band) are cleanly resolved. The fraction of the total 5′-FAM-labeled DNA that is covalently bound shows a hyperbolic response to increasing enzyme concentrations for each DNA substrate.

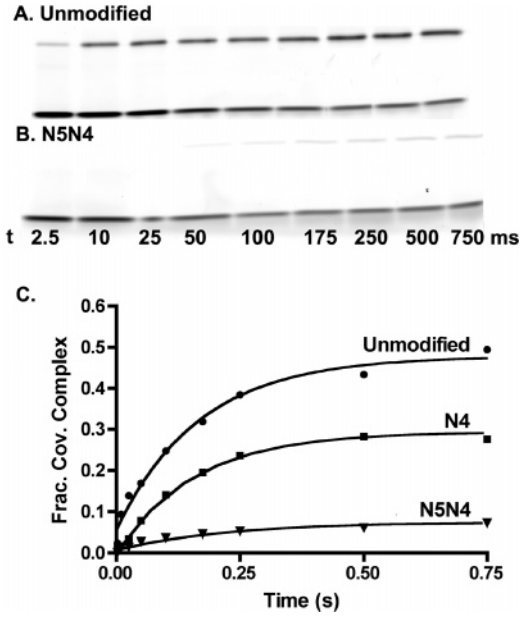

FIGURE 4: Approach-to-equilibrium cleavage kinetics with the FAM32AP/32-mer duplex DNA. (A and B) SDS−PAGE gels showing the time course for reaction of vTopo with unmodified and doubly modified (N5N4) DNA. These reactions were performed in a rapid mix−chemical quench apparatus. The top band in each gel is the E−S covalent complex, whereas the bottom band is the free DNA. (C) The fraction of covalent complex at each time point was fitted to a first-order rate expression to obtain the observed cleavage rate ($k_{obsd} = k_{cl} + k_r$).

However, the substituted sequences show large decreases in the amount of covalently bound DNA at a saturating concentration of vTopo as compared to the native consensus sequence (Figure 3E).

Analysis of the equilibrium cleavage data using eq 1 established that these substitutions have little effect on the binding constant (K_D) but that the internal cleavage equilibrium (K_{cl}) decreased to a varying extent depending on the substitution. The binding constant for the unmodified FAM-32AP/32-mer was 120 ± 50 nM, whereas those of the substituted DNA sequences differed by less than 2-fold from this value. On the other hand, the cleavage equilibrium for the N5 and N4 substrates was ~3-fold smaller than that of the native sequence [K_{cl}(native) = 1.6 ± 0.3]. Moreover, the cleavage equilibrium constants for the H5H4, H5H3, N5N4, and N5N3 doubly modified sequences were 3−16-fold lower than that of the consensus sequence (see Discussion). A complete analysis of the effects on K_D and K_{cl} for all the modifications is presented in the Discussion.

Approach-to-Equilibrium Cleavage Kinetics (k_{cl}). The cleavage rate constant for each FAM32AP/32-mer equilibrium cleavage substrate was measured using a rapid mix−chemical quench instrument. The enzyme and substrate were rapidly mixed, and the reactions were quenched with 10% SDS at various time intervals before separation of the covalently bound DNA product by denaturing polyacrylamide gel electrophoresis (Figure 4A,B). In this analysis, the fraction of covalent complex increases over time until the equilibrium level is reached. The amount of covalent complex at the end point for each of these reactions was indistinguishable from that observed in the equilibrium cleavage measurements (compare Figure 3E with Figure 4C), which establishes that equilibrium was obtained within the time frame of these measurements. The fraction of covalent complex as a function of time was fitted to a first-order rate equation to obtain the observed rate for the approach to equilibrium ($k_{obs} = k_{cl} + k_r$). Despite the large effects of some substitutions on K_{cl}, the cleavage rates were surprisingly unaffected in nearly all cases (Table 1). The only significant exceptions were the double modifications B2B1 and N4B1, in which k_{cl} was increased 2- and 2.5-fold, respectively, and the substrates H5H3 and N5N4, which showed k_{cl} values 2.4- and 11-fold smaller, respectively, than that of the consensus sequence (Table 1).

DNA Ligation Rate Constants (k_r). The rates of DNA ligation (k_r) were calculated from the cleavage equilibrium constant and the observed rate of cleavage using the equality $k_r = k_{obs}/(K_{cl} + 1)$. For the unmodified FAM32AP/32-mer, $k_r = 1.1 \pm 0.14\ s^{-1}$. Except for the purine (P) singly modified DNA at positions 1 and 2, every other modified DNA was found to increase the religation rate, providing the primary kinetic explanation for the decrease in the cleavage equilibrium constant observed for these modified substrates (see Table 1). The increase in k_r was more significant for the G site substitutions (up to 5-fold) as compared to the A site alterations, highlighting the primary significance of the G sites.

DISCUSSION

Specific enzymatic recognition of the DNA major groove can take advantage of hydrogen bonding groups that are displayed within this structural feature of B-DNA. With respect to the vTopo nonscissile strand consensus sequence, 3′-GGGAA-5′, the G sites present lone pair hydrogen bond acceptors on the N7 and O6 positions, and the A sites present an acceptor site at N7 and a donor site at the 6-amino group (Figure 2). These potential interaction sites have been removed using four different unnatural bases. Two of these, 7-deazaguanine (H) and 7-dezaadenine (B), are very subtle modifications that selectively remove the lone pair electrons at position 7 without disrupting any other aspect of the base pair. In contrast, 2-aminopurine (N) and purine (P) substitutions remove the O6 and 6-NH_2 groups, respectively, but also disrupt base pairing at the G and A sites, respectively. Thus, interpretation of the energetic effects of the N and P substitutions must be made more guardedly than for the more conservative H and B substitutions. Finally, introduction of simultaneous modifications at two sites allows one to ask the question of whether energetic communication exists between interaction sites. In other words, is the interaction at site one energetically unchanged, enhanced, or weakened when the interaction at site two is removed? The strength of these enzyme−DNA contacts can be quantified at each step of the vTopo reaction to reveal important elements of catalytic specificity.

Single-G Site Modifications. The effects of single N and H major groove modifications on K_D, K_{cl}, k_{cl}, and k_r are summarized in Table 1. The major effect of these G site modifications is a decrease in K_{cl} of as much as 4-fold, with smaller effects on K_D. The largest outcomes are seen at positions 4 and 5 with the 7-deaza (H) substitutions, suggesting that the enzyme donates a hydrogen bond with N7 of G^{+4} and G^{+5}. Substitution of G^{+4} and G^{+5} with N also decreases K_{cl} by a comparable amount (N lacks the O6

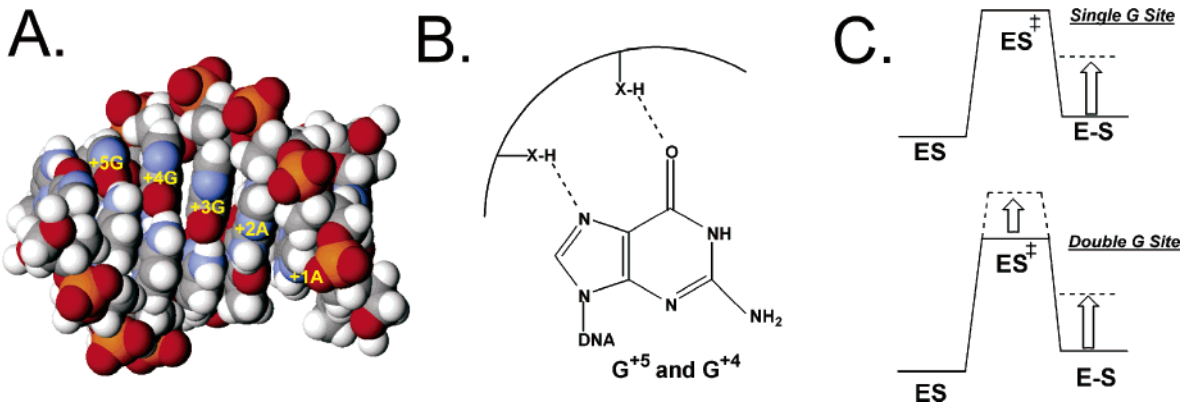

FIGURE 5: Consensus sequence major groove interactions of vTopo and energetic effects of single- and double-G site modifications. (A) Space filling model of duplex DNA containing the consensus sequence. The view is looking into the major groove where the O6 and N7 hydrogen bond-accepting groups of the three guanine bases are displayed. (B) Hydrogen bond interactions of vTopo with G^{+5} and G^{+4} as inferred from H and N substitution at these sites. (C) Energetic effect of single- and double-site G modifications. The single-site modification has an effect on only the ground state covalent complex, while the double-site modification has an effect on both the ground state covalent complex and the transition state (see the text).

atom of guanine). Because previous studies have found that inosine substitution at these positions had no effect on the cleavage equilibrium (inosine lacks the 2-amino group of guanine) (*7*), these findings suggest that vTopo donates hydrogen bonds to both the N7 and O6 acceptor groups of the guanines at positions 4 and 5 but that the 2-amino group is not an important recognition element (Figure 5A,B). Smaller effects are seen when these same substitutions are made at the guanine at position 3, a result that is consistent with previous findings where this position was found to be fairly tolerant to both inosine and adenine substitutions (*7*).

Corresponding kinetic studies with this series of singly substituted equilibrium substrates establish that the decreases in K_{cl} arise almost entirely from increases in the ligation rate (k_r) with no large changes in k_{cl} (Table 1). This result indicates that the N7 and O6 single-site deletions increase the ligation rate by selectively destabilizing the covalent complex without affecting the stability of the transition state for cleavage and ligation. This conclusion is based on the requirement that energetic perturbations to the transition state for cleavage and ligation must be manifested as equal changes in k_{cl} and k_r, which is not observed. These results contrast with the approximately 150-fold decreases in the cleavage rate observed when entire bases were deleted form positions 3 and 4 (*19*).[2] Possible mechanisms for the selective increases in the ligation rate induced by these modified bases are considered below.

Double-G Site Modifications. For the most part, the cleavage equilibrium constants for the double-site N and H modifications are reduced from that of the two single modifications by an amount that is expected from independent, multiplicative effects on this equilibrium constant (i.e., additive effects of the two interaction free energies). Surprisingly, the simple multiplicative effects of the double modifications on the cleavage equilibrium mask substantial nonmultiplicative effects on the kinetic constants k_{cl} and k_r. The H5H3, N5N4, and N5N3 substrates exhibit large decreases in k_{cl}, whereas the calculated multiplicative effects of the two single modifications are small (Table 1). This outcome is the hallmark of energetic cooperativity in the transition state, possibly arising from significant structural changes in the complex brought about by the combined removal of two N7 or O6 hydrogen bond acceptor groups. In contrast to the unexpected decreases in k_{cl}, the combined modifications give rise to increases in k_r much smaller than what would be expected on the basis of multiplicative effects of the single modifications (Table 1). The different results on the two rate constants can be simply rationalized if the double modifications destabilize the transition state and covalent complex to similar extents, leading to only small changes in the activation barrier for ligation but significant increases in the activation barrier for cleavage.

As summarized in the free energy diagrams in Figure 5C, removal of single N7 or O6 atoms at positions 5, 4, and 3 selectively destabilizes the covalent complex, thereby enhancing the rate of ligation. In contrast, double modifications show equal destabilizing effects in the transition state and covalent complex leading to slower rates of cleavage and less damaging effects on ligation.

A Site Modifications. Small changes in K_D, K_{cl}, k_{cl}, and k_r are seen upon single and double 7-deaza and purine substitution at A^{+2} and A^{+1} (Table 1). Interestingly, purine (P) substitution has little effect at the A^{+2} and A^{+1} positions, indicating that the exocyclic amino group of adenine is not an important recognition element. This finding sheds light on previous work in which inosine substitutions at positions 1 and 2 were found to abrogate cleavage entirely (*7*). This large effect is likely due to the nonconservative nature of the inosine substitution that replaces the 6-amino group of adenine with a carbonyl group. In contrast, the more subtle P substitution used here simply removes the amino group

[2] Although increases in the religation rate, with no significant decreases in the cleavage rate, are observed with the 32/32-mer equilibrium substrates substituted at positions 3−5, we do observe 1.5−4-fold decreases in the rate of irreversible strand cleavage using similarly substituted 18/24-mer suicide cleavage substrates. The results with the suicide substrates are consistent with the previous base ablation studies of the Shuman group (i.e., cleavage rate decreases) (*19*). The apparent discrepancy between the effects of major groove alterations using suicide and equilibrium substrates arises from anticooperative interactions between the GGGAA major groove and the downstream DNA regions that are present in the equilibrium substrate and absent in the suicide substrate (R. Nagarajan and J. T. Stivers, unpublished observations). A comprehensive study of anticooperativity in DNA strand binding, cleavage, and religation by vTopo is in progress.

(Figure 2). In summary, the N7 and exocyclic amino groups of the A sites are not critical recognition elements.

Combined G and A Site Modifications. To investigate whether there is energetic coupling between the G and A sites of the consensus sequence, H3B1 and N4B1 doubly modified DNAs were synthesized and their activity with vTopo was measured. As observed for the other substrates, both H3B1 and N4B1 double modifications produced small effects on K_D (Table 1). Although the K_{cl} value for the N4B1 substrate was only modestly smaller than that of the consensus sequence, and within a factor of 2 of that anticipated from multiplication of the two single effects, this "null" effect on K_{cl} was brought about by significant and equal increases in both k_{cl} and k_r (Table 1). The H3B1 modification differs in that significant nonmultiplicative effects on K_{cl} were observed that arise from antagonism of the two H3 and B1 modifications on the religation rate. Minimally, these results indicate that the G and A sites can energetically communicate and that combined changes in both sites can give rise to kinetic outcomes different from those with combined modifications within the G site alone (see above).

Specificity Mechanisms and the Importance of Positioning the Phosphotyrosine Linkage in Topoisomerase Reactions. Ensemble and single-molecule measurements have established that vTopo removes multiple DNA supercoils during the lifetime of each covalent intermediate (*9*, *10*). A hallmark of this type of mechanism is that strand ligation and rotation are competitive kinetic processes. In other words, the lifetime of the covalent complex determines how many supercoils are removed after a single cleavage event. The free rotation mechanism for supercoil release places limits on the mechanisms that vTopo may employ to obtain specificity (i.e., the relative number of supercoils removed from a specific site and a nonspecific site in a given length of time). We consider three possible specificity mechanisms and their outcomes.

(1) Sequence-specific interactions could be used by the enzyme to selectively stabilize the transition state for cleavage and ligation. Although such a mechanism would increase the rate of covalent complex formation, it would also be antagonistic with a free rotation mechanism for supercoil release, because the rate of ligation would also increase. We conclude that such interactions cannot in themselves substantially enhance specificity for DNA relaxation because the lifetime of the covalent complex is decreased, and thus, fewer supercoils are removed per cleavage event.

(2) Sequence-specific interactions could be used by the enzyme to selectively destabilize (strain) the ground state noncovalent complex, thereby lowering the activation barrier for cleavage. Sequence-specific contacts such as this could give rise to substantial specificity only if the contacts became stronger in the covalent complex (release of strain). This is required because equal ground state strain in both complexes is energetically equivalent to transition state stabilization which has been discussed in ref *1*.

(3) vTopo could use sequence-specific interactions to selectively stabilize the ground state covalent complex, thereby increasing its lifetime. In the case of an infinitely stable covalent complex, every rate-limiting cleavage event would lead to complete relaxation of a DNA molecule. This type of mechanism could lead to substantial specificity, especially if balanced with ground state strain in the noncovalent complex and/or transition state stabilization. Of course, an infinitely stable covalent adduct is not compatible with successful replication of DNA, because the enzyme-induced strand nicks would be converted into double-strand breaks when encountered by a replication fork. Indeed, excessive stabilization of the covalent complex is the poisoning mechanism of the clinically useful topoisomerase drugs (*20*). Thus, the lifetime of the covalent adduct is limited by this intrinsic biological constraint.

On the basis of the considerations mentioned above, we envision that sequence-specific DNA interactions are in part used to optimize the stability of the covalent complex and thereby enhance specificity for supercoil release. Thus, even the subtle major groove perturbations investigated here can have measurable effects on adduct lifetime. What is the physical basis for such sequence-specific effects on the stability of the covalent complex? Since most of the effects manifest themselves in the ground state for religation, it is probable that these major groove interactions are used to optimally position the phosphotyrosine target with respect to the 5′-hydroxyl nucleophile. Since the 5′-hydroxyl needs to freely rotate to remove supercoils, it is unlikely that topoisomerase rigidly positions this group. Instead, it seems more likely that the relative position (or mobility) of the phosphotyrosine center determines the efficiency of religation. If this center is too close to the trajectory of the rotating 5′-OH nucleophile, then religation occurs too frequently. Alternatively, if the phosphotyrosine group is rigidly held too far away, religation never occurs. Thus, one use of sequence-specific interactions is to carefully position the phosphotyrosine moiety relative to the rotating nucleophile such that frequent ligations or overly stable strand nicks are prevented.

REFERENCES

1. Shuman, S., and Prescott, J. (1990) Specific DNA cleavage and binding by vaccinia virus DNA topoisomerase I, *J. Biol. Chem. 265*, 17826−36.
2. Shuman, S. (1991) Site-specific interaction of vaccinia virus topoisomerase I with duplex DNA. Minimal DNA substrate for strand cleavage in vitro, *J. Biol. Chem. 266*, 20576−7.
3. Shuman, S. (1991) Site-specific DNA cleavage by vaccinia virus DNA topoisomerase I. Role of nucleotide sequence and DNA secondary structure, *J. Biol. Chem. 266*, 1796−803.
4. Sekiguchi, J., and Shuman, S. (1994) Vaccinia topoisomerase binds circumferentially to DNA, *J. Biol. Chem. 269*, 31731−4.
5. Cheng, C., and Shuman, S. (1999) Site-specific DNA transesterification by vaccinia topoisomerase: Role of specific phosphates and nucleosides, *Biochemistry 38*, 16599−612.
6. Yakovleva, L., Handy, C. J., Sayer, J. M., Pirrung, M., Jerina, D. M., and Shuman, S. (2004) Benzo[*c*]phenanthrene adducts and nogalamycin inhibit DNA transesterification by vaccinia topoisomerase, *J. Biol. Chem. 278*, 42170−7.
7. Shuman, S., and Turner, J. (1993) Site-specific interaction of vaccinia virus topoisomerase I with base and sugar moieties in duplex DNA, *J. Biol. Chem. 268*, 18943−50.
8. Tian, L., Claeboe, C. D., Hecht, S. M., and Shuman, S. (2004) Remote phosphate contacts trigger assembly of the active site of DNA topoisomerase IB, *Structure 12*, 31−40.
9. Koster, D. A., Croquette, V., Dekker, C., Shuman, S., and Dekker, N. H. (2005) Friction and torque govern the relaxation of DNA supercoils by eukaryotic topoisomerase IB, *Nature 434*, 671−4.
10. Stivers, J. T., Harris, T. K., and Mildvan, A. S. (1997) Vaccinia DNA topoisomerase I: Evidence supporting a free rotation mechanism for DNA supercoil relaxation, *Biochemistry 36*, 5212−22.

11. Nagarajan, R., Kwon, K., Nawrot, B., Stec, W. J., and Stivers, J. T. (2005) Catalytic phosphoryl interactions of topoisomerase IB, *Biochemistry 44*, 11476−85.
12. Sekiguchi, J., and Shuman, S. (1995) Proteolytic footprinting of vaccinia topoisomerase bound to DNA, *J. Biol. Chem. 270*, 11636−45.
13. Sekiguchi, J., and Shuman, S. (1996) Covalent DNA binding by vaccinia topoisomerase results in unpairing of the thymine base 5′ of the scissile bond, *J. Biol. Chem. 271*, 19436−42.
14. Sekiguchi, J., and Shuman, S. (1996) Identification of contacts between topoisomerase I and its target DNA by site-specific photocrosslinking, *EMBO J. 15*, 3448−57.
15. Yakovleva, L., Tian, L., Sayer, J. M., Kalena, G. P., Kroth, H., Jerina, D. M., and Shuman, S. (2003) Site-specific DNA transesterification by vaccinia topoisomerase: Effects of benzo[α]-pyrene-dA, 8-oxoguanine, 8-oxoadenine and 2-aminopurine modifications, *J. Biol. Chem. 278*, 42170−7.
16. Kwon, K., and Stivers, J. T. (2002) Fluorescence spectroscopy studies of vaccinia type IB DNA topoisomerase. Closing of the enzyme clamp is faster than DNA cleavage, *J. Biol. Chem. 277*, 345−52.
17. Stivers, J. T., Jagadeesh, G. J., Nawrot, B., Stec, W. J., and Shuman, S. (2000) Stereochemical outcome and kinetic effects of R_p- and S_p-phosphorothioate substitutions at the cleavage site of vaccinia type I DNA topoisomerase, *Biochemistry 39*, 5561−72.
18. Kwon, K., Jiang, Y. L., Song, F., and Stivers, J. T. (2002) ^{19}F NMR studies of vaccinia type IB topoisomerase. Conformational dynamics of the bound DNA substrate, *J. Biol. Chem. 277*, 353−8.
19. Tian, L., Sayer, J. M., Jerina, D. M., and Shuman, S. (2004) Individual nucleotide bases, not base pairs, are critical for triggering site-specific DNA cleavage by vaccinia topoisomerase, *J. Biol. Chem. 279*, 39718−26.
20. Liu, L. F. (1989) DNA topoisomerase poisons as antitumor drugs, *Annu. Rev. Biochem. 58*, 351−75.

BI060133I